Chapter III.4

Colliders for particle physics

Oliver Brüning [a], *Massimo Giovannozzi* [a], *John Jowett* [a,b], *Elias Métral* [a], *Louis Rinolfi* [a,c], *Todd Satogata* [d], *Daniel Schulte* [a] *and Frank Zimmermann* [a]

[a] CERN, Geneva Switzerland

[b] GSI Helmholtzzentrum für Schwerionenforschung GmbH, Darmstadt, Germany

[c] European Scientific Institute, Archamps, France

[d] Jefferson Lab, Newport News, VA, USA

This chapter includes a short introduction on colliders with their main figure of merit, the luminosity, and the pile-up in the experiments' detectors, followed by seven sections, offering an overview of the different types of colliders used for particle physics experiments, which have been discussed during the past JUAS schools:

– LHC and HL-LHC,
– Nuclear collisions at the LHC,
– The Future CERN Circular hadron collider (FCC-hh),
– Electron-positron circular colliders,
– Future high-energy linear lepton colliders,
– The US Electron-Ion Collider,
– Muon collider.

III.4.1 Introduction

Elias Métral

CERN, Geneva, Switzerland

At the end of an acceleration chain, particle accelerators can be used in two modes, the fixed-target mode and the collider mode (see Fig. III.4.1) and the first role of the beam energy is to produce new particles through Einstein's relation $E = mc^2$, with E the total particle energy, m the relativistic mass and c the speed of light. The huge advantage of the collider mode is that the energy available in the centre-of-mass (CM), to create new particles, is much higher than the one from an accelerator working in fixed-target mode. This can be easily seen starting from the relativistic invariant with one particle

$$E^2 - p^2c^2 = E_0^2 \quad , \tag{III.4.1}$$

This chapter should be cited as: Colliders for particle physics, E. Métral *et al.*, DOI: 10.23730/CYRSP-2024-003.1925, in: Proceedings of the Joint Universities Accelerator School (JUAS): Courses and exercises, E. Métral (ed.), CERN Yellow Reports: School Proceedings, CERN-2024-003, DOI: 10.23730/CYRSP-2024-003, p. 1925.

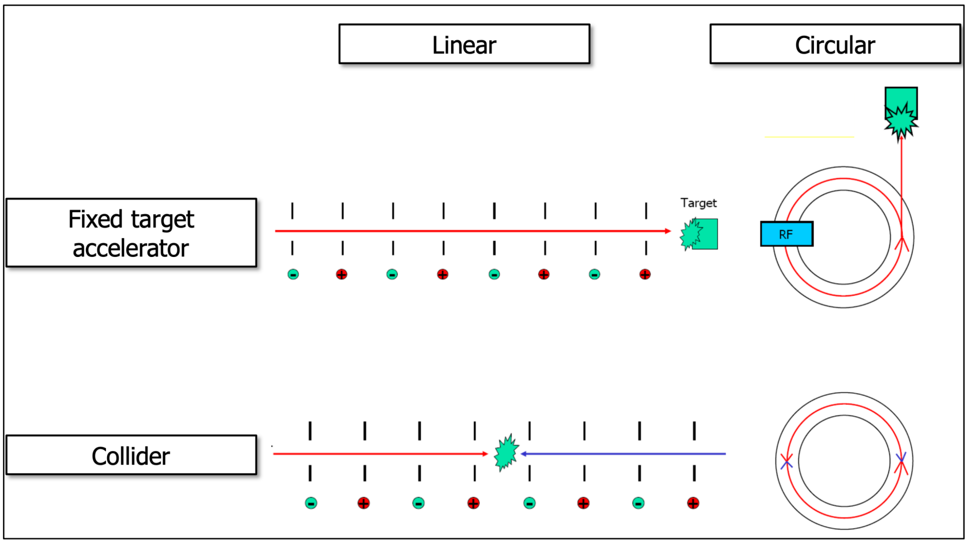

Fig. III.4.1: The two modes of operation of linear or circular particle accelerators (at the end of an acceleration chain): fixed-target mode and collider mode.

where p is the momentum and $E_0 = m_0 c^2$ is the rest energy (with m_0 the rest mass). The same result is obtained for any isolated system, composed of e.g. two particles called 1 and 2, which will collide [1]

$$(E_1 + E_2)^2 - (\vec{p_1} + \vec{p_2})^2 c^2 = (\text{invariant mass})^2 c^4 \quad . \tag{III.4.2}$$

In this case, the available energy in the CM, E_{CM} (also written sometimes $\sqrt{s}$), is thus given by

$$E_{\text{CM}} = \sqrt{s} = \sqrt{(E_1 + E_2)^2 - (\vec{p_1} + \vec{p_2})^2 c^2} \quad , \tag{III.4.3}$$

which can be rewritten as

$$E_{\text{CM}} = \sqrt{m_{01}^2 c^4 + m_{02}^2 c^4 + 2(E_1 E_2 - \vec{p_1}.\vec{p_2} c^2)} \quad , \tag{III.4.4}$$

with m_{01} and m_{02} the rest masses of the particles 1 and 2. It can then be deduced from Eq. (III.4.4) that for an accelerator working in fixed-target mode (for which $\vec{p_2} = 0$) at sufficiently high energy (i.e. such that the rest masses can be neglected)

$$E_{\text{CM,FT}} = \sqrt{2 E_1 m_{02} c^2} \quad , \tag{III.4.5}$$

whereas for a collider colliding similar particles (for which $\vec{p_2} = -\vec{p_1}$),

$$E_{\text{CM,C}} = E_1 + E_2 = 2E_1 \quad . \tag{III.4.6}$$

Comparing Eqs. (III.4.5) and (III.4.6), it can be concluded that, to have the same energy as in the CM of a collider colliding similar particles, the energy required for the accelerator working in fixed-target mode

E_{FT} is given by

$$E_{\mathrm{FT}} = 2\gamma_{\mathrm{C}} E_{\mathrm{C}} \quad , \tag{III.4.7}$$

where γ_{C} and E_{C} are the relativistic mass factor and total (one) beam energy of the collider. In the CERN LHC, for instance, $\gamma_{\mathrm{C}} \approx 7460$ and therefore $2\gamma_{\mathrm{C}} \approx 15\,000$. This means that the beam energy of the accelerator working in fixed-target mode should be $\sim 15\,000$ times higher than the beam energy of the LHC (of 7 TeV), i.e. it should be ~ 100 PeV. This figure explains the considerable advantage of using colliders for particle discoveries and for precision measurements.

The second role of the beam energy is to resolve the inner structure of matter through de Broglie's relation $E = hc/\lambda$, with h the Planck's constant and λ the associated wave length. The wave length should be smaller than the dimension of the object to be resolved (see Table III.4.1).

Table III.4.1: The second role of the beam energy: resolve the inner structure of matter.

	Object's size [m]	**Energy needed [GeV]**
Atom	$\sim 10^{-10}$	$\sim 10^{-5}$
Nucleus	$\sim 10^{-14}$	$\sim 10^{-1}$
Nucleon	$\sim 10^{-15}$	~ 1
Quark	$\sim 10^{-18}$	$\sim 10^{3}$
< Quark	$\sim 10^{-19}$	$\sim 10^{4}$

It is worth reminding that accelerators contributed to twenty-six Nobel Prizes in physics since 1939, as can be seen in Fig. III.4.2, and a short history of colliders is summarised in Fig. III.4.3. It can be observed in particular that both linear and circular colliders have been built to collide hadrons or leptons or both. In a hadron collider, the simplest case is to collide protons, each made of three quarks. Such a collider is used to study the frontier of physics, it is a discovery machine with collisions of several quarks with not all nucleon energy available in collision and a huge background. On the contrary, a lepton collider is used for precision physics, it is a study machine with elementary particles collisions and a well-defined CM energy per elementary constituent. As concerns the limitations, the hadron colliders are limited by the dipole field available and the ring size (reminder: p [GeV/c] ≈ 0.3 B [T] ρ [m], with B the magnetic induction and ρ the dipole bending radius) and therefore the way forward is to go to higher magnetic fields or/and larger circumferences. The lepton colliders are limited by the energy lost from synchrotron radiation (reminder: $U_{\mathrm{lost}} \propto E^4/\rho E_0^4$) and therefore, there, the way forward is to go to large diameter circular colliders, linear colliders or heavier leptons (such as muons).

The main figure of merit of a collider is its luminosity [2, 3]. The number of events generated per unit time $N_{\mathrm{exp/time}}$ (which is given by the detector) is the product of the reaction cross-section of interest σ_{exp} (which is given by nature) and the (instantaneous) luminosity L (which is given by the collider)

$$N_{\mathrm{exp/time}} = \sigma_{\mathrm{exp}} L \quad , \tag{III.4.8}$$

and the total number of events N_{exp} is given by

Accelerators contributed to 26 Nobel Prizes in physics since 1939

- 1939 Ernest O. Lawrence
- 1951 John D. Cockcroft & Ernest Walton
- 1952 Felix Bloch
- 1957 Tsung-Dao Lee & Chen Ning Yang
- 1959 Emilio G. Segrè & Owen Chamberlain
- 1960 Donald A. Glaser
- 1961 Robert Hofstadter
- 1963 Maria Goeppert Mayer
- 1967 Hans A. Bethe
- 1968 Luis W. Alvarez
- 1976 Burton Richter & Samuel C.C. Ting
- 1979 Sheldon L. Glashow, Abdus Salam & Steven Weinberg
- 1980 James W. Cronin & Val L. Fitch
- 1981 Kai M. Siegbahn
- 1983 William A. Fowler
- 1984 Carlo Rubbia & Simon van der Meer
- 1986 Ernst Ruska
- 1988 Leon M. Lederman, Melvin Schwartz & Jack Steinberger
- 1989 Wolfgang Paul
- 1990 Jerome I. Friedman, Henry W. Kendall & Richard E. Taylor
- 1992 Georges Charpak
- 1995 Martin L. Perl
- 2004 David J. Gross, Frank Wilczek & H. David Politzer
- 2008 Makoto Kobayashi & Toshihide Maskawa
- 2013 François Englert & Peter Higgs
- 2015 Takaaki Kajita & Arthur B. MacDonald

Fig. III.4.2: Nobel Prizes in physics linked to particle accelerators since 1939 (Courtesy of P. Lebrun).

- 1943, R. Widerøe patents the concept of colliding beams in storage rings
- 1961, the first electron-positron storage ring AdA is built in Frascati
- 1971, CERN starts operating the ISR, first proton-proton collider
- 1982, the CERN SPS is converted into a proton-antiproton collider
- 1987, the TeVatron at Fermilab is converted into a proton-antiproton collider
- 1987, the SSC, a 40 TeV proton-proton collider, is approved for construction in the USA. The project was subsequently cancelled in 1993.

- 1989, CERN starts operating the 26.7 km, high-energy electron-positron collider LEP
- 1989, SLAC starts operating the SLC, first linear collider converted from the linac
- 1991, HERA at DESY becomes the first proton-electron collider
- 1999, RHIC at BNL becomes the first heavy-ion collider
- 2008, CERN starts operation of the LHC, 14 TeV proton-proton collider
- 2012, design studies are published for electron-positron linear colliders, ILC and CLIC
- 2014, CERN launches design study for Future Circular Colliders (100 km circumference)

Fig. III.4.3: Some milestones in the history of colliders (Courtesy of P. Lebrun).

$$N_{\mathrm{exp}} = \sigma_{\mathrm{exp}} \int L(t)dt = \sigma_{\mathrm{exp}} L_{\mathrm{int}} \quad , \tag{III.4.9}$$

with L_{int} the integrated luminosity. By definition, the luminosity L is the time-averaged integral over the interaction volume V of the number of reactions per unit time and volume and it is given by

$$L = \frac{1}{T_{\mathrm{b}}} \int_0^{T_{\mathrm{b}}} \int_V S dt dV \quad , \tag{III.4.10}$$

where T_{b} is the bunch collision period ($T_{\mathrm{b}}^{-1} = f_{\mathrm{b}} = f_0 M$ with f_0 the revolution period and M the number of bunches) and S is the luminosity density. Considering two bunches of particles with densities

ρ_1 and ρ_2 (both normalised to one), the luminosity density is given by

$$S = N_1 N_2 \rho_1(x,y,s,t)\rho_2(x,y,s,t) M_{\mathrm{KLF}} \quad , \tag{III.4.11}$$

where N_1 and N_2 are the numbers of particles per bunch for beams 1 and 2, while M_{KLF} is the Møller Kinematic Luminosity factor [4], given by

$$M_{\mathrm{KLF}} = \sqrt{(\vec{v_1} - \vec{v_2})^2 - \frac{(\vec{v_1} \times \vec{v_2})^2}{c^2}} \quad , \tag{III.4.12}$$

with $\vec{v}_{1,2}$ the velocities of beams 1 and 2 in the laboratory frame. The first term of M_{KLF} corresponds to the natural (nonrelativistic) case and the second term is a correction factor that makes S a relativistic invariant. Combining Eqs. (III.4.10) and (III.4.11), yields

$$L = M N_1 N_2 f_0 M_{\mathrm{KLF}} \int_0^{T_{\mathrm{b}}} \int_V \rho_1(x,y,s,t)\rho_2(x,y,s,t) dt dV \quad . \tag{III.4.13}$$

Changing the time variable from time t to s_0, with $s_0 = ct$, Eq. (III.4.13) can be rewritten (see also Figs. III.4.4 and III.4.5)

$$L = M N_1 N_2 f_0 \frac{M_{\mathrm{KLF}}}{c} \int\int\int\int \rho_1(x,y,s,-s_0)\rho_2(x,y,s,s_0) dx dy ds ds_0 \quad . \tag{III.4.14}$$

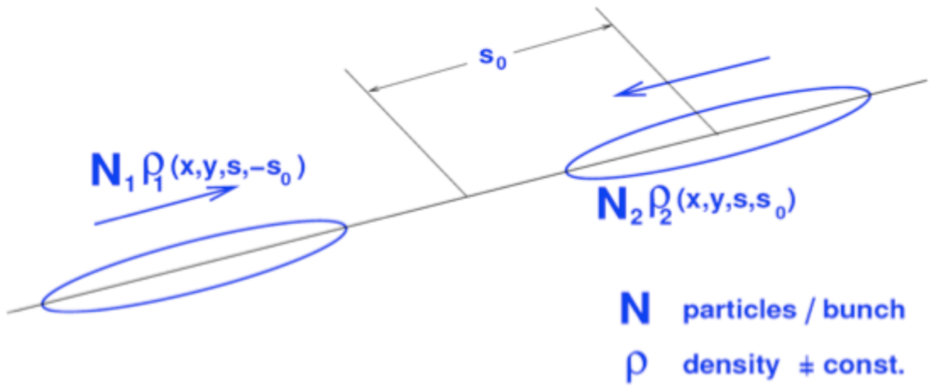

Fig. III.4.4: Collisions without crossing angle (Courtesy of W. Herr).

Using a frame such that in Fig. III.4.5, the x-axis points to the top of the page, the y-axis points towards the reader and the s-axis points to the right of the page, M_{KLF} can be written as

$$\frac{M_{\mathrm{KLF}}}{c} = \sqrt{\beta_1^2 + \beta_2^2 + 2\beta_1\beta_2 \cos\Phi - \beta_1^2\beta_2^2 \sin^2\Phi} \quad , \tag{III.4.15}$$

where β_1 and β_2 are the relativistic velocity factors for beams 1 and 2 respectively. In case $\beta_1 = \beta_2 = 1$, Eq. (III.4.15) becomes

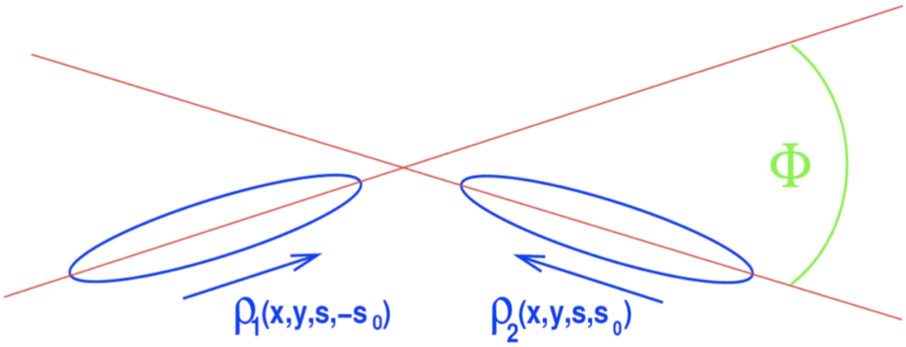

Fig. III.4.5: Collisions with crossing angle (Courtesy of W. Herr).

$$\frac{M_{\mathrm{KLF}}}{c} = 2\cos^2\frac{\Phi}{2} \quad , \tag{III.4.16}$$

which simplifies to 2 when $\Phi = 0$ (i.e. in the absence of crossing angle).

Let's assume first the simplest case without crossing angle ($\Phi = 0$), then Eq. (III.4.14) becomes

$$L = MN_1N_2f_0 2\int\int\int\int \rho_1(x,y,s,-s_0)\rho_2(x,y,s,s_0)dxdydsds_0 \quad . \tag{III.4.17}$$

Assuming then that the densities are uncorrelated in all planes, i.e. $\rho_1(x,y,s,-s_0) = \rho_{1x}(x)\rho_{1y}(y)\rho_{1s}(s-s_0)$ and $\rho_2(x,y,s,s_0) = \rho_{2x}(x)\rho_{2y}(y)\rho_{2s}(s+s_0)$, given by Gaussian distributions in all dimensions, Eq. (III.4.17) becomes

$$L = \frac{2MN_1N_2f_0}{(2\pi)^3\sigma_{1x}\sigma_{1y}\sigma_{2x}\sigma_{2y}}\int\int\int\int \frac{e^{-\frac{x^2}{2\sigma_{1x}^2}}e^{-\frac{y^2}{2\sigma_{1y}^2}}e^{-\frac{x^2}{2\sigma_{2x}^2}}e^{-\frac{y^2}{2\sigma_{2y}^2}}e^{-\frac{(s-s_0)^2}{2\sigma_{1s}^2}}e^{-\frac{(s+s_0)^2}{2\sigma_{2s}^2}}}{\sigma_{1s}\sigma_{2s}}dxdydsds_0 \quad . \tag{III.4.18}$$

Assuming $\sigma_{1s} = \sigma_{2s} = \sigma_s$, yields

$$L = \frac{MN_1N_2f_0}{4\pi^2\sigma_{1x}\sigma_{1y}\sigma_{2x}\sigma_{2y}}\int\int e^{-\frac{x^2}{2\sigma_{1x}^2}}e^{-\frac{y^2}{2\sigma_{1y}^2}}e^{-\frac{x^2}{2\sigma_{2x}^2}}e^{-\frac{y^2}{2\sigma_{2y}^2}}dxdy \quad , \tag{III.4.19}$$

using the relation $\int\int \frac{e^{-\frac{s^2}{\sigma_s^2}}e^{-\frac{s_0^2}{\sigma_s^2}}}{\sigma_s^2}dsds_0 = \pi$. Finally, assuming also $\sigma_{1x} = \sigma_{2x} = \sigma_x$ and $\sigma_{1y} = \sigma_{2y} = \sigma_y$ and using the relation $\int\int \frac{e^{-\frac{x^2}{\sigma_x^2}}e^{-\frac{y^2}{\sigma_y^2}}}{\sigma_x\sigma_y}dxdy = \pi$, yields the simplest formula for the (instantaneous) luminosity in the case of head-on collisions, which we call L_0,

$$L_0 = \frac{MN_1N_2f_0}{4\pi\sigma_x\sigma_y} \quad . \tag{III.4.20}$$

In the case of round beams ($\sigma_x = \sigma_y = \sigma$) of equal number of particles ($N_1 = N_2 = N_\mathrm{b}$), Eq. (III.4.20) simplifies even further to

$$L_0 = \frac{M N_\mathrm{b}^2 f_0 \beta\gamma}{4\pi\beta^* \epsilon_\mathrm{n}} \quad , \tag{III.4.21}$$

where β and γ are the relativistic velocity and mass factors of the two beams, β^* is the betatron function at the collision point (also called Interaction Point, IP) and ϵ_n is the normalised transverse beam emittance given by

$$\epsilon_\mathrm{n} = \beta\gamma\epsilon = \beta\gamma\frac{\sigma^2}{\beta^*} \quad . \tag{III.4.22}$$

As an example, the numerical application for the nominal case of the CERN LHC gives $L_0 = 1.2 \times 10^{34}$ cm^{-2} s^{-1}. Now that we defined the simplest scenario, let's have a closer look to more complicated cases, noting that, in the general case, the luminosity is given by

$$L = L_0 F \quad , \tag{III.4.23}$$

with $0 \leq F \leq 1$.

A crossing angle is often needed to separate the two counter-rotating beams in the part of the machine where they share the same vacuum chamber, to avoid unwanted collisions outside of the detector (see Fig. III.4.6). Furthermore, the exact (minimum) crossing angle is defined after careful analyses of the long-range beam-beam effects (see Fig. III.4.7).

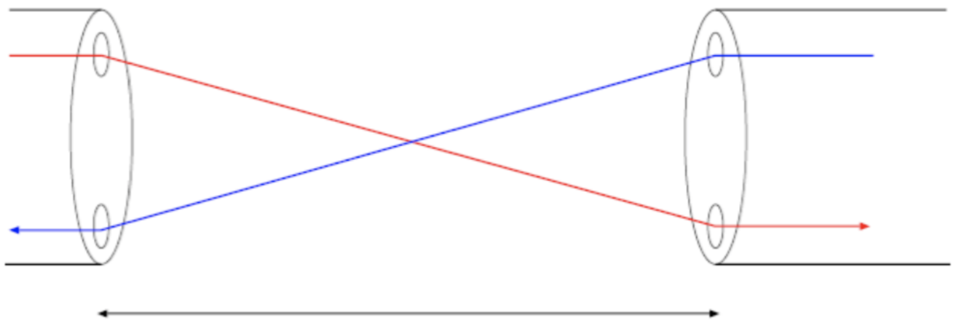

Fig. III.4.6: The two counter-rotating beams of the CERN LHC sharing the same vacuum chamber for ~ 120 m around the IP (Courtesy of W. Herr).

In the case of a crossing angle (CA) in the s-x plane, beam 1 is rotated by $\Phi/2$ while beam 2 is rotated by $-\Phi/2$ and the luminosity can be written as

$$L_\mathrm{CA} = 2\cos^2\frac{\Phi}{2} M N_1 N_2 f_0 \int\int\int\int \rho_{1x}(x_1)\rho_{1y}(y_1)\rho_{1s}(s_1-s_0)\rho_{2x}(x_2)\rho_{2y}(y_2)\rho_{2s}(s_2+s_0)dxdydsds_0 \quad , \tag{III.4.24}$$

with

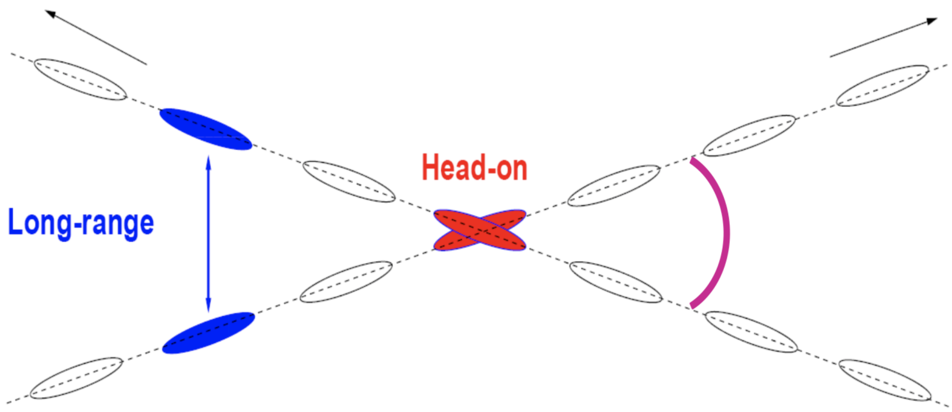

Fig. III.4.7: The two beam-beam effects when the two counter-rotating beams share the same vacuum chamber (Courtesy of W. Herr).

$$\begin{bmatrix} x_1 \\ s_1 \end{bmatrix} = \begin{bmatrix} \cos\frac{\Phi}{2} & -\sin\frac{\Phi}{2} \\ \sin\frac{\Phi}{2} & \cos\frac{\Phi}{2} \end{bmatrix} \begin{bmatrix} x \\ s \end{bmatrix} \quad , \tag{III.4.25}$$

and

$$\begin{bmatrix} x_2 \\ s_2 \end{bmatrix} = \begin{bmatrix} \cos\frac{\Phi}{2} & \sin\frac{\Phi}{2} \\ -\sin\frac{\Phi}{2} & \cos\frac{\Phi}{2} \end{bmatrix} \begin{bmatrix} x \\ s \end{bmatrix} \quad . \tag{III.4.26}$$

Assuming the same dimensions in the three planes, i.e. $\sigma_{1x} = \sigma_{2x} = \sigma_x$, $\sigma_{1y} = \sigma_{2y} = \sigma_y$, $\sigma_{1s} = \sigma_{2s} = \sigma_s$ and $y_1 = y_2 = y$, and using the following relation

$$\int_{-\infty}^{+\infty} e^{-(at^2+bt+c)} dt = \sqrt{\frac{\pi}{a}} e^{\frac{b^2}{4a}-c} \quad , \tag{III.4.27}$$

it can be shown that

$$L_{\mathrm{CA}} = L_0 F_{\mathrm{CA}} \quad , \tag{III.4.28}$$

with

$$F_{\mathrm{CA}} = \frac{1}{\sqrt{1 + (\frac{\sigma_s}{\sigma_x} \tan\frac{\Phi}{2})^2}} \quad . \tag{III.4.29}$$

Figure III.4.8 depicts the evolution of the luminosity reduction factor from a crossing angle as a function of the longitudinal rms bunch length. It is worth noting that this geometric luminosity loss factor can be compensated by using crab cavities (see Fig. III.4.9), as it has been already the case in some leptons machine (KEK-B in Japan) and as it will be the case for the future upgrade of the LHC (the HL-LHC [5]).

In the presence of a transverse offset (TO) between the two beams, e.g. in the horizontal plane, but without crossing angle, using the same frame as before one has, in the general case, $x_1 = x + d_1$ and

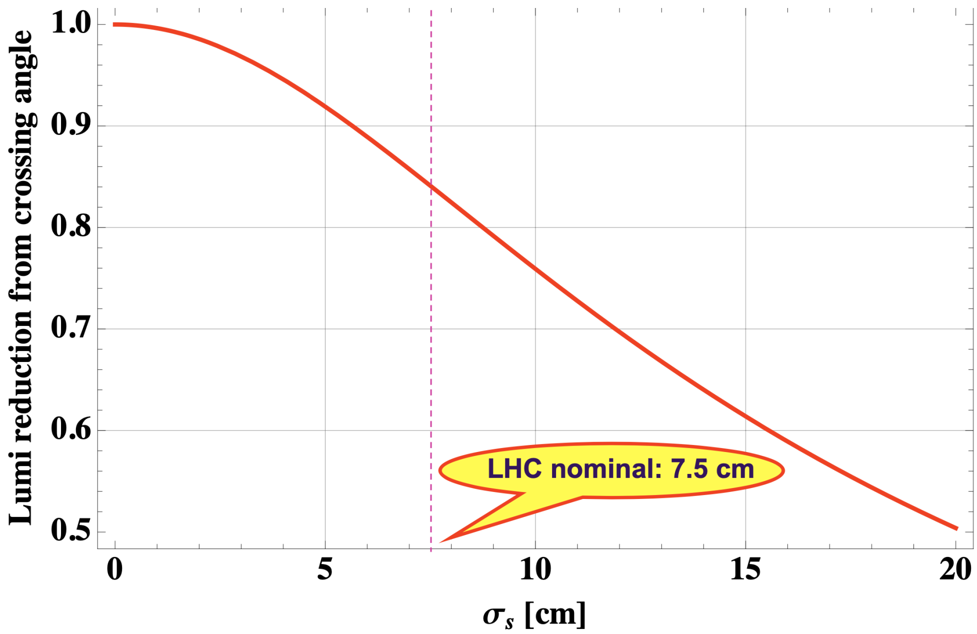

Fig. III.4.8: Evolution of the luminosity reduction factor from a crossing angle as a function of the rms bunch length (example of the nominal LHC).

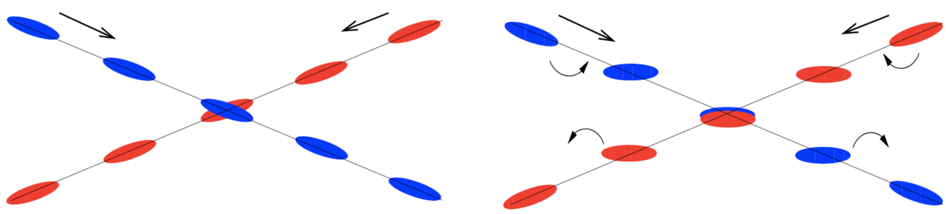

Fig. III.4.9: (Left) Collisions with a crossing angle; (right) compensation of the crossing angle at the IP by crab cavities (Courtesy of W. Herr).

$x_2 = x + d_2$. Making again the assumptions $\sigma_{1x} = \sigma_{2x} = \sigma_x$, $\sigma_{1y} = \sigma_{2y} = \sigma_y$, $\sigma_{1s} = \sigma_{2s} = \sigma_s$ and $y_1 = y_2 = y$ yields

$$L_{\text{TO}} = L_0 F_{\text{TO}} \quad , \tag{III.4.30}$$

with

$$F_{\text{TO}} = e^{-(\frac{d_1 - d_2}{2\sigma_x})^2} \quad . \tag{III.4.31}$$

The evolution of the luminosity reduction factor as a function of the transverse beam offset is depicted in Fig. III.4.10.

Another important effect, called the hourglass effect (HE), needs to be taken into account when β^* is comparable or smaller than the rms bunch length σ_s, remembering that close to the IP, the variation of the betatron function is given by

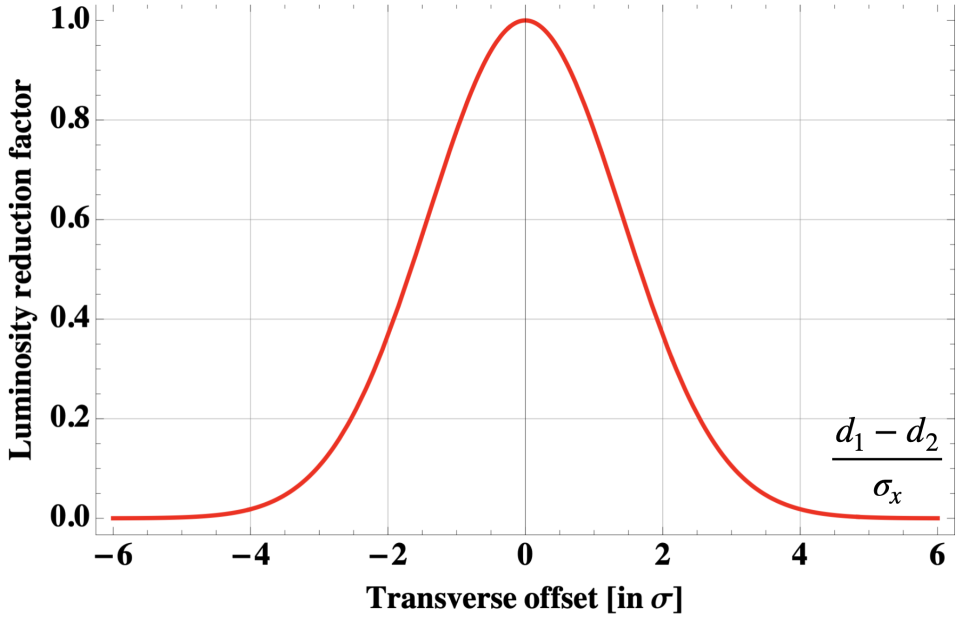

Fig. III.4.10: Evolution of the luminosity reduction factor as a function of the transverse beam offset.

$$\beta(s) = \beta^*[1 + (\frac{s}{\beta^*})^2] \quad . \tag{III.4.32}$$

Following the same approach as before, considering also the presence of a crossing angle in the s-x plane but no transverse offset, yields

$$L_{\mathrm{CA-HG}} = L_{\mathrm{CA}} F_{\mathrm{HG}} \quad , \tag{III.4.33}$$

with

$$F_{\mathrm{HG}} = \sqrt{\frac{\frac{\sin^2\frac{\Phi}{2}}{\sigma_x^{*2}} + \frac{\cos^2\frac{\Phi}{2}}{\sigma_s^2}}{\pi}} \int_{-\infty}^{+\infty} \frac{e^{-s^2\{\frac{\sin^2\frac{\Phi}{2}}{\sigma_x^{*2}[1+(\frac{s}{\beta^*})^2]} + \frac{\cos^2\frac{\Phi}{2}}{\sigma_s^2}\}}}{1 + (\frac{s}{\beta^*})^2} ds \quad . \tag{III.4.34}$$

The evolution of the luminosity reduction factor as a function of β^* is depicted in Fig. III.4.11, where it can indeed be checked that this effect starts to become important when β^* is comparable or smaller than the rms bunch length σ_s.

It is worth reminding here that the luminosity L depends only on the beam parameters and that it is independent of the physical reaction. It is given by the ratio between the number of events per second generated in the collisions and the cross-section of the reaction under study and therefore its unit is $\mathrm{cm}^{-2}\,\mathrm{s}^{-1}$. It is computed by the accelerator physicists using the formulae described above and measured by the particle physicists. As the luminosity is directly proportional to the interaction rate, luminosity measurements are usually based on fast counting devices which provide such a signal.

As we saw from Eq.III.4.9, the maximisation of the integrated luminosity L_{int} is what matters in

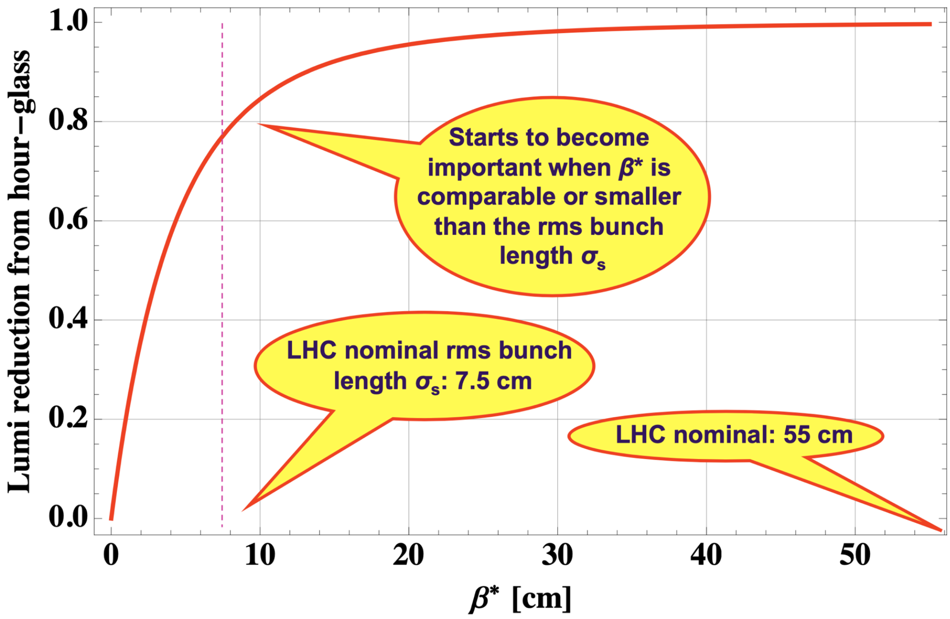

Fig. III.4.11: Evolution of the luminosity reduction factor from the hourglass effect as a function of β^* (example of the nominal LHC).

the end as it gives the maximum number of events. Collisions in a high-luminosity collider result in a continuous burn-off of the circulating beams, which is the dominant effect that reduces the instantaneous luminosity over time. Some other effects like emittance growth can also reduce it and let's assume for simplicity an exponential decay of the instantaneous luminosity given by

$$L(t) = L_{\text{peak}} e^{-\frac{t}{\tau_{\text{l}}}} \quad , \tag{III.4.35}$$

where L_{peak} is the (peak) luminosity at the beginning of the collisions (one often speaks of a "fill" during which the collider experts declare "stable beams" and the experiments take their data) and τ_{l} the luminosity lifetime. Then, the question is: what is the best run time t_{r}? To answer this question, let's call t_{p} the preparation time (time needed to put the beams in collision after the end of the previous physics fill). The average luminosity is thus given by

$$< L >= \frac{1}{t_{\text{r}} + t_{\text{p}}} \int_0^{t_{\text{r}}+t_{\text{p}}} L(t) dt = L_{\text{peak}} \tau_{\text{l}} \frac{1 - e^{-\frac{t_{\text{r}}}{\tau_{\text{l}}}}}{t_{\text{r}} + t_{\text{p}}} \quad , \tag{III.4.36}$$

which is maximum (optimum) for

$$t_{\text{r}}^{\text{opt}} \approx \tau_{\text{l}} \ln\left(1 + \sqrt{2\frac{t_{\text{p}}}{\tau_{\text{l}}}} + \frac{t_{\text{p}}}{\tau_{\text{l}}}\right) \quad . \tag{III.4.37}$$

A numerical example is shown in Fig. III.4.12 with τ_{l} = 15 h and t_{p} = 10 h, for which it can be deduced from Eq. (III.4.37) that the optimum run time is $t_{\text{r}}^{\text{opt}} \approx$ 15.5 h (in good agreement with Fig. III.4.12).

The nuclear unit of the cross-section (σ_{exp}) is the barn, with 1 barn = 10^{-24} cm^2, and the in-

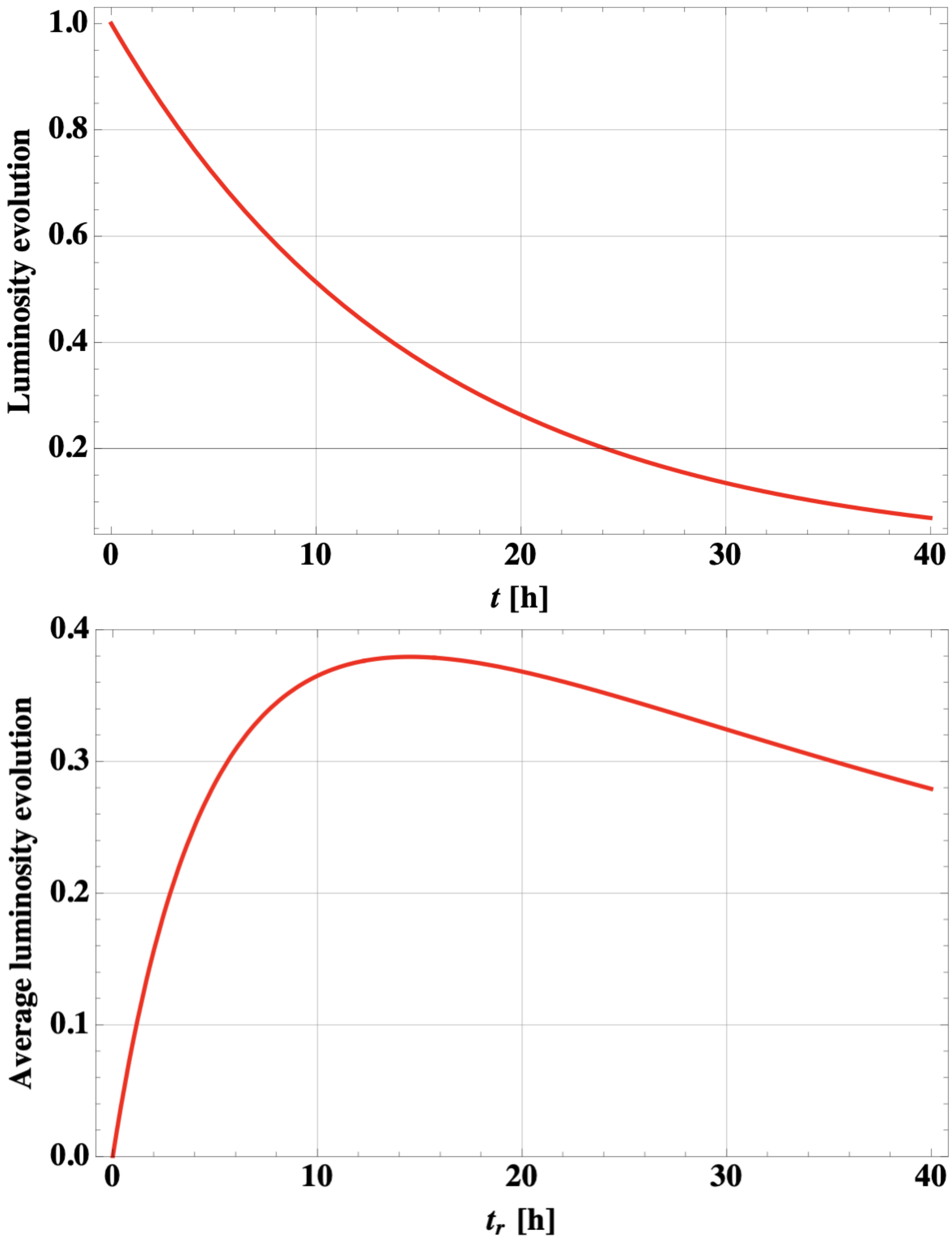

Fig. III.4.12: Numerical example of maximisation of the integrated luminosity, with (top) the evolution of the luminosity with time and (bottom) the evolution of the average luminosity with the run time t_r (example of the nominal LHC). Here, τ_l = 15 h and t_p = 10 h.

verse femtobarn (fb^{-1}) is the unit typically used to measure the number of particle collision events per femtobarn of target cross-section and is the conventional unit for time-integrated luminosity. Thus, if a detector has accumulated 100 fb^{-1} of integrated luminosity, one expects to find 100 events per femtobarn of cross-section within these data. As an example, Fig. III.4.13 shows the evolution of the integrated and peak luminosities over the years for the CERN LHC .

Another important consideration for the experiments is the pile-up (PU), which describes the number of events per crossing for a given luminosity and is given by

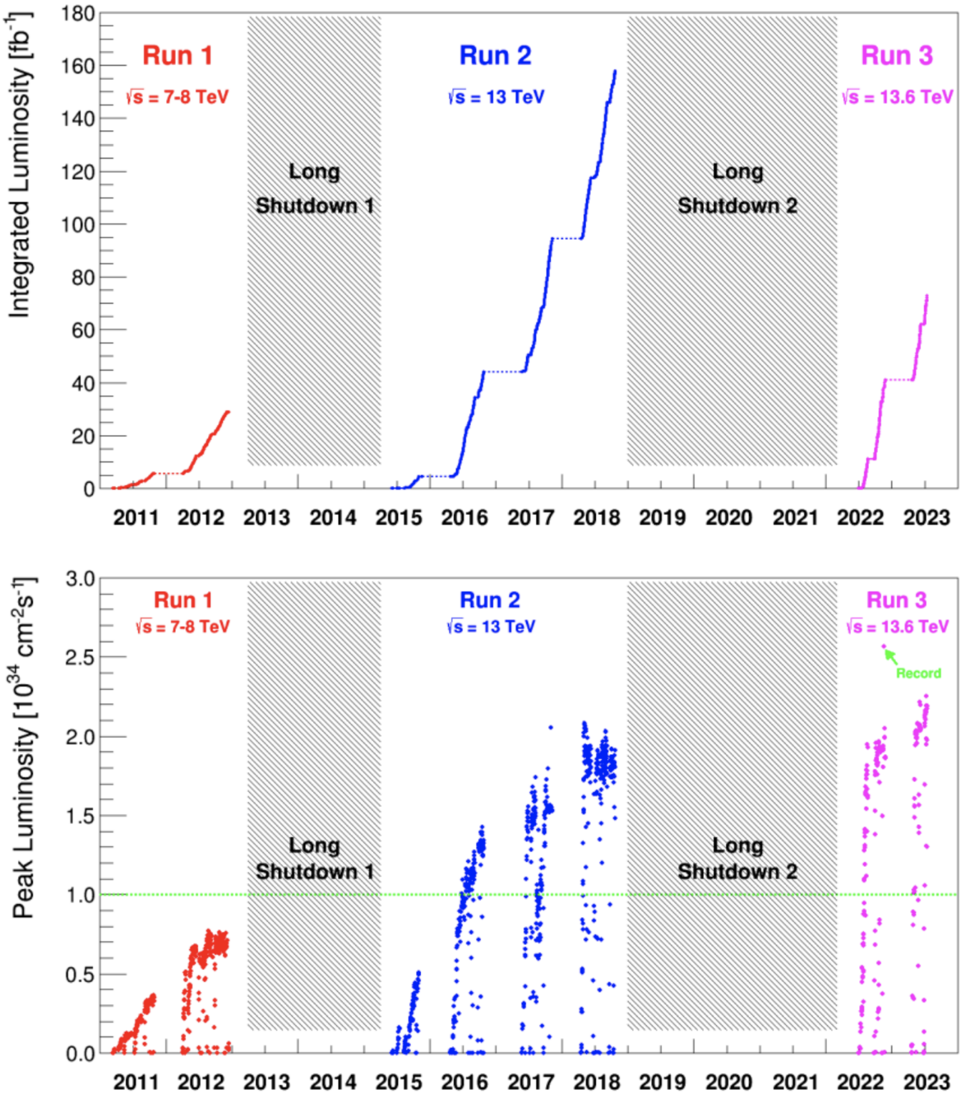

Fig. III.4.13: Integrated and peak luminosities over the years for the CERN LHC.

$$\mathrm{PU} = \frac{L\sigma_{\mathrm{exp}}}{M f_0} \quad . \tag{III.4.38}$$

This is a limit coming from the experiments' detectors and is thus better to have the largest number of bunches for the same beam intensity. In case the PU is too big (for instance it was ~ 20 for the CERN LHC with nominal parameters and it should reach 200 for the ultimate HL-LHC), luminosity-leveling techniques can be used to remain at the limit, playing with the different parameters which can reduce the luminosity (transverse beam offset, β^*, etc.).

In summary, to reach a high luminosity, we need

- High beam intensities,
  - A high bunch intensity is more efficient (for the same beam intensity) but it can lead to a PU issue for the experiments' detectors

  – A high number of bunches is less efficient but better for the PU

– Small transverse beam sizes (small transverse emittance and beta function at the IP),
– High energy,
– Small crossing angle,
– Small transverse offset,
– Short bunches.

Finally, to conclude this introduction on particle colliders, it is worth emphasising the current six major challenges for the future high-energy colliders, which are

– Synchrotron radiation,
– Bending magnetic fields,
– Accelerating gradient,
– Particle production (positrons, antiprotons, muons),
– Power consumption and sustainability,
– Cost.

References

[1] R. Hagedorn, Relativistic kinematics: a guide to the kinematic problems of high-energy physics (W.A. Benjamin, New York, NY, 1964, Internet Archive.

[2] M.A. Furman *et al.*, Luminosity, in *Handbook of accelerator physics and engineering*, 3rd ed., Eds. A.W. Chao *et al.* (World Scientific, Singapore, 2023), pp. 367–374, doi:10.1142/9789811269189_0004.

[3] W. Herr and B. Muratori, Concept of luminosity, in Proc. CAS-CERN Accelerator School: Intermediate Accelerator Physics, 15–26 Sep. 2003, Zeuthen, Germany, edited by D. Brand, CERN-2006-002 (CERN, Geneva, 2006), pp.361–378, doi:10.5170/CERN-2006-002.361.

[4] M.A. Furman, The Møller luminosity factor, LBNL-53553, CBP Note-543 (Lawrence Berkeley National Laboratory, Berkeley, 2003), doi:10.2172/836235.

[5] O. Brüning and L. Rossi (Eds.), The High Luminosity Large Hadron Collider: The new machine for illuminating the mysteries of Universe (World Scientific, Singapore, 2015), doi:10.1142/9581.